

Qilong Wang,¹ Miao Zhang,² Gloria Torres,¹ Shengnan Wu,¹ Changan Ouyang,¹ Zhonglin Xie,¹ and Ming-Hui Zou¹



Metformin Suppresses Diabetes-Accelerated Atherosclerosis via the Inhibition of Drp1-Mediated Mitochondrial Fission

Diabetes 2017;66:193–205 | DOI: 10.2337/db16-0915

Metformin is a widely used antidiabetic drug that exerts cardiovascular protective effects in patients with diabetes. How metformin protects against diabetes-related cardiovascular diseases remains poorly understood. Here, we show that metformin abated the progression of diabetes-accelerated atherosclerosis by inhibiting mitochondrial fission in endothelial cells. Metformin treatments markedly reduced mitochondrial fragmentation, mitigated mitochondrial-derived superoxide release, improved endothelial-dependent vasodilation, inhibited vascular inflammation, and suppressed atherosclerotic lesions in streptozotocin (STZ)-induced diabetic ApoE^{-/-} mice. In high glucose-exposed endothelial cells, metformin treatment and adenoviral overexpression of constitutively active AMPK downregulated mitochondrial superoxide, lowered levels of dynamin-related protein (Drp1) and its translocation into mitochondria, and prevented mitochondrial fragmentation. In contrast, AMPK- α 2 deficiency abolished the effects of metformin on Drp1 expression, oxidative stress, and atherosclerosis in diabetic ApoE^{-/-}/AMPK- α 2^{-/-} mice, indicating that metformin exerts an antiatherosclerotic action in vivo via the AMPK-mediated blockage of Drp1-mediated mitochondrial fission. Consistently, mitochondrial division inhibitor 1, a potent and selective Drp1 inhibitor, reduced mitochondrial fragmentation, attenuated oxidative stress, ameliorated endothelial dysfunction, inhibited inflammation, and suppressed atherosclerosis in diabetic mice. These findings show that metformin attenuated the development of atherosclerosis by reducing Drp1-mediated mitochondrial fission in an AMPK-dependent manner.

Suppression of mitochondrial fission may be a therapeutic approach for treating macrovascular complications in patients with diabetes.

Patients with diabetes exhibit accelerated atherosclerosis compared with patients without diabetes. Hyperglycemia in diabetes is believed to exacerbate atherosclerosis by promoting the release of reactive oxygen species (ROS) that damage sensitive cell components, such as DNA, cause premature cell death, and reduce nitric oxide (NO) availability, thus resulting in endothelial dysfunction (1). Several ROS-producing systems, including NADPH oxidases, uncoupled endothelial NO synthase (eNOS), and mitochondria, contribute to ROS generation (2). Increased mitochondrial ROS are critical for the initiation of endothelial dysfunction and the acceleration of atherosclerosis in diabetes (3). For example, overexpression of mitochondrial thioredoxin 2 or administration of the mitochondria-targeted antioxidant, mitoQ, reduces atherosclerotic lesions in ApoE^{-/-} mice (4,5).

Mitochondria are critical integrators of energy production, ROS generation, signaling transduction, and apoptosis. Recent work has highlighted the importance of mitochondrial dynamics, particularly mitochondrial fusion and fission, in mitochondrial homeostasis (6). Mitochondrial fusion seems to be beneficial because it distributes metabolites, proteins, and DNA throughout the mitochondrial network. In contrast, excessive mitochondrial fission may be detrimental because it causes the

¹Center for Molecular and Translational Medicine, Georgia State University, Atlanta, GA

²Department of Medicine, The University of Oklahoma Health Sciences Center, Oklahoma City, OK

Corresponding author: Ming-Hui Zou, mzou@gsu.edu, or Zhonglin Xie, zxie@gsu.edu.

Received 26 July 2016 and accepted 6 October 2016.

This article contains Supplementary Data online at <http://diabetes.diabetesjournals.org/lookup/suppl/doi:10.2337/db16-0915/-/DC1>.

Q.W. and M.Z. contributed equally to this work.

© 2017 by the American Diabetes Association. Readers may use this article as long as the work is properly cited, the use is educational and not for profit, and the work is not altered. More information is available at <http://www.diabetesjournals.org/content/license>.

accumulation of fragmented mitochondria with electron transport chain (ETC) impairment and increases mitochondrial ROS in mammalian cells (7,8). In endothelial cells, mitochondrial fission also contributes to the reduction in eNOS-derived NO bioavailability (9), impairment of angiogenesis (10), and induction of apoptosis (11). Furthermore, an increase in mitochondrial fission is associated with the pathogenesis of diabetic cardiomyopathy (12), nephropathy (13), and peripheral neuropathy (14).

A recent work reported that high glucose induces mitochondrial fission by upregulating dynamin-related protein (Drp1) protein expression (15). Drp1 is a cytosolic guanosine-5'-triphosphatase that triggers mitochondrial division by binding with fission 1 (Fis1) or mitochondrial fission factor (Mff) on mitochondria. The increased mitochondrial fission contributes to diabetes-induced endothelial dysfunction (9). These studies suggest that the suppression of mitochondrial fission may effectively prevent diabetes-induced atherosclerosis and its related cardiovascular complications.

Metformin is a synthetic dimethyl biguanide and has been a mainstay of therapy for patients with type 2 diabetes mellitus (T2DM). In addition to lowering blood glucose, metformin reduces cardiovascular complications in patients with diabetes (16). For instance, it prevents the progression of common carotid intima-media thickness, an indicator of atherosclerosis, and reduces the incidence of myocardial infarction in patients with T2DM (17,18). These beneficial cardiovascular effects appear to be independent of its antihyperglycemic effect, because other conventional treatments (e.g., insulin and sulfonylurea) exhibit less beneficial cardiovascular effects.

Increasing evidence has shown that metformin inhibits mitochondrial fragmentation by activating AMPK in diabetes (15,19), resulting in the prevention of endothelial damage such as apoptosis and inflammation (20–22). Similarly, fish oil is an AMPK activator that regulates the expression of mitochondrial dynamics-related proteins, including mitofusin 2 (MFN2) and Fis1, accompanied with a reduction in atherosclerotic plaques in ApoE^{-/-} mice fed a high-fat diet (23). Furthermore, vascular smooth muscle cells (VSMCs) isolated from atherosclerotic arteries of ApoE^{-/-} mice express low levels of MFN2 (24). Although the above-mentioned events indicate the potential role of MFN2 in atherosclerosis, whether mitochondrial fission directly promotes the development of atherosclerosis is unknown, and whether this mechanism is involved in the antiatherosclerotic action of metformin in diabetes remains unclear.

Using streptozotocin (STZ)-induced diabetic ApoE^{-/-} mice, we found that metformin reduced Drp1 expression and Drp1-mediated mitochondrial fission in an AMPK-dependent manner. Moreover, inhibition of mitochondrial fission by metformin or mitochondrial division inhibitor 1 (mdivi-1) attenuated diabetes-induced oxidative stress, endothelial dysfunction, and atherosclerosis development.

RESEARCH DESIGN AND METHODS

The Georgia State University Institutional Animal Care and Use Committee reviewed and approved the animal protocols in this study.

Animal Experiments

C57BL/6J wild-type (WT) mice were obtained from The Jackson Laboratory (Bar Harbor, ME). AMPK- $\alpha 2^{-/-}$ /ApoE^{-/-} mice were generated as previously described (25). ApoE^{-/-} littermates served as controls. Mice were housed in temperature-controlled cages under a cycle with 12 h of light and 12 h of darkness.

Eight-week-old male WT mice were intraperitoneally injected with 50 mg/kg STZ for 5 days, according to the Animal Models of Diabetic Complications Consortium protocol. Blood glucose was assayed 2 weeks after injection with the OneTouch Ultra Blood Glucose Monitoring System (LifeScan Inc., Wayne, PA). Mice with blood glucose >300 mg/dL were considered to have diabetes. Diabetic mice were treated 1 month later with insulin (0.5 units/kg, twice per day, intraperitoneally, 14 days), mdivi-1 (1.2 mg/kg/d, osmotic pump, 14 days), or metformin (300 mg/kg/d, drinking water, 4 weeks). At the end of the experiments, aortas were collected for endothelial function, ROS production, and Western blot analyses.

In another set of experiments, 8-week-old male ApoE^{-/-} and AMPK- $\alpha 2^{-/-}$ /ApoE^{-/-} mice were fed the chow diet. Diabetes was induced by STZ injection, as previously described. Diabetic mice were treated 2 weeks later with metformin (300 mg/kg/d in drinking water, 12 weeks) or mdivi-1 (10 mg/kg, intraperitoneally, twice per week, 8 weeks). At the end of the experiments, aortas were collected for immunohistochemistry, immunofluorescent, and Western blot analyses.

Reagents

Mdivi-1, STZ, D-glucose, mannitol, and insulin were purchased from Sigma-Aldrich (St. Louis, MO). Metformin was obtained from Spectrum Chemical Manufacturing Corp. (New Brunswick, NJ). Primary antibodies information (name, company, catalog number, molecular weight) are provided in Supplementary Table 1. All other chemicals used were of the highest commercial grade available.

Atherosclerosis Studies

Aortic root lesions and en face lesions of the aortic arch were stained with Sudan IV and Oil Red O, respectively, as described previously (26). Serum cholesterol and triglyceride levels were determined using Infinity reagent (Thermo Fisher Scientific).

Assessment of ROS Production

To assess mitochondrial ROS production, we incubated freshly isolated aortic rings with 2 μ mol/L MitoSOX Red (Thermo Fisher Scientific) in Krebs buffer at 37°C for 20 min. The aortic rings were homogenized in 50% methanol (100 μ L) with a glass pestle. Tissue homogenates were passed through a 0.22- μ m syringe filter, and the methanol filtrates were injected into a Waters HPLC

e2695 separation module to separate and quantify the MitoSOX oxidation product, mito-2-hydroxyethidium, with a Waters 2475 fluorescence detector at excitation and emission wavelengths of 510 and 580 nm, respectively. Human umbilical vein endothelial cells (HUVECs) were incubated with endothelial basal medium (EBM) containing 2 $\mu\text{mol/L}$ MitoSOX Red for 30 min. The cells were rinsed twice with PBS, mounted in SHUR/Mount medium, and observed by the Olympus BX53F microscope. Intracellular ROS in freshly isolated aortas were measured using dihydroethidium (DHE; Thermo Fisher Scientific) as described previously (27).

Measurement of Endothelial Function

Vessel bioactivity was assayed by organ chamber (Radnoti LLC, Monrovia, CA), as described previously (28). Mouse descending aortic rings were precontracted with 30 nmol/L U46619. At the plateau of contraction, endothelium-dependent and -independent vasodilation responses were determined in the presence of acetylcholine (ACh; 10^{-9} to 10^{-5} mol/L) or sodium nitroprusside (SNP; 10^{-10} to 10^{-6} mol/L), respectively.

Immunohistochemistry and Immunofluorescence

Immunohistochemical staining was performed on thoracic aortas to detect Drp1, 3-nitrotyrosine (3-NT), intracellular adhesion molecule 1 (ICAM-1), and vascular cell adhesion molecule 1 (VCAM-1) as described previously (28). For 8-oxo-2'-deoxyguanosine (8-OHdG) staining, aortic sections were pretreated with proteinase K and RNase A before incubation with the primary antibody. The semiquantitative analysis of tissue staining was performed using an arbitrary grading system from a score of 0 to 5 (score 0: no staining; score 1: 1–20%; score 2: 21–40%; score 3: 41–60%; score 4: 61–80%; and score 5: 81–100% positive staining in the intima).

Immunofluorescent staining was performed on aortic root to detect ICAM-1 and VCAM-1 (29). The grade of fluorescence intensity for ICAM-1 and VCAM-1 was measured using ImageJ software (National Institutes of Health).

Cell Culture

HUVECs were obtained from American Type Culture Collection (Manassas, VA) and grown in EBM medium with growth supplement (Gibco). Cells were incubated at 37°C in a humidified atmosphere of 5% CO₂ and 95% air and grown to 70–80% confluence. Cells at passages three to eight were used in the experiments.

Immunoblotting

Western blotting was performed using the standard method, as previously described (30).

Quantification of Mitochondrial Morphology

HUVECs were seeded and grown on glass coverslips (MatTek Corp.). Mitochondrial morphology was visualized by incubating the cells with MitoTracker Deep Red (excitation: 644 nm; Invitrogen) for 30 min. Cells were transferred into an incubation chamber (37°C, 5% CO₂), and images were acquired using LSM-800 time-lapse

confocal microscopy with $\times 40$ oil immersion objective lens. Z-stacks of thresholded images were volume reconstructed using the VolumeJ plug-in (31). We can track changes in mitochondrial size that ranged from 0.039 to 0.873 μm^2 . The number and individual volume of each mitochondrion were analyzed and quantified using the ImageJ 3D Object Counter plug-in. At least 100 cells were analyzed in each sample to determine cells undergoing mitochondrial fragmentation. A decrease in mitochondrial volume and an increase in the number of mitochondria per cell were considered as mitochondrial fission.

Statistical Analysis

Values are expressed as mean \pm SEM. One- or two-way ANOVA was used to compare the differences among three or more groups, followed by Bonferroni multiple comparison tests using GraphPad Prism 5 software (GraphPad Software, Inc., La Jolla, CA). Values of $P < 0.05$ were considered significant.

RESULTS

Metformin Reduces Atherosclerotic Lesions in Diabetic ApoE^{-/-} Mice but Not in Diabetic ApoE^{-/-}/AMPK- α 2^{-/-} Mice

Compared with nondiabetic ApoE^{-/-} mice, diabetic ApoE^{-/-} mice developed significantly larger en face lesions in the aortic arches and more atherosclerotic lesions in the aortic sinus. Metformin treatment (300 mg/kg/d in drinking water, 16 weeks) significantly reduced lesion areas in the aortic root and aortic arch in diabetic ApoE^{-/-} mice but not in nondiabetic ApoE^{-/-} mice (Fig. 1A–D).

Metformin exerts its cardiovascular protective role by activating AMPK (28,32). To explore whether AMPK is involved in the antiatherosclerotic action of metformin in the context of diabetes, we backcrossed AMPK- α 2-deficient mice onto an ApoE^{-/-} background to generate ApoE^{-/-}/AMPK- α 2^{-/-} mice. Diabetic ApoE^{-/-}/AMPK- α 2^{-/-} mice developed more atherosclerotic lesions in the aortic sinus and aortic arch compared with nondiabetic ApoE^{-/-}/AMPK- α 2^{-/-} mice. Metformin administration attenuated the development of atherosclerosis in diabetic ApoE^{-/-} mice but did not reduce the development of atherosclerotic lesions in diabetic ApoE^{-/-}/AMPK- α 2^{-/-} mice (Fig. 1A–D). We further determined the effect of metformin on AMPK in these mice by evaluating the phosphorylation of AMPK at Thr-172. Metformin treatment increased the phosphorylation of AMPK in ApoE^{-/-} mouse aortas but not in ApoE^{-/-}/AMPK- α 2^{-/-} mouse aortas (Fig. 1E).

We also measured whether metformin affects serum lipid and glucose metabolism in STZ-induced diabetic mice (Supplementary Table 2). Diabetic ApoE^{-/-} and diabetic ApoE^{-/-}/AMPK- α 2^{-/-} mice showed lower body weights and higher blood glucose and serum cholesterol levels than nondiabetic mice. However, there was no difference in these metabolic parameters between mice with and without metformin treatment. These results suggest that metformin may decrease

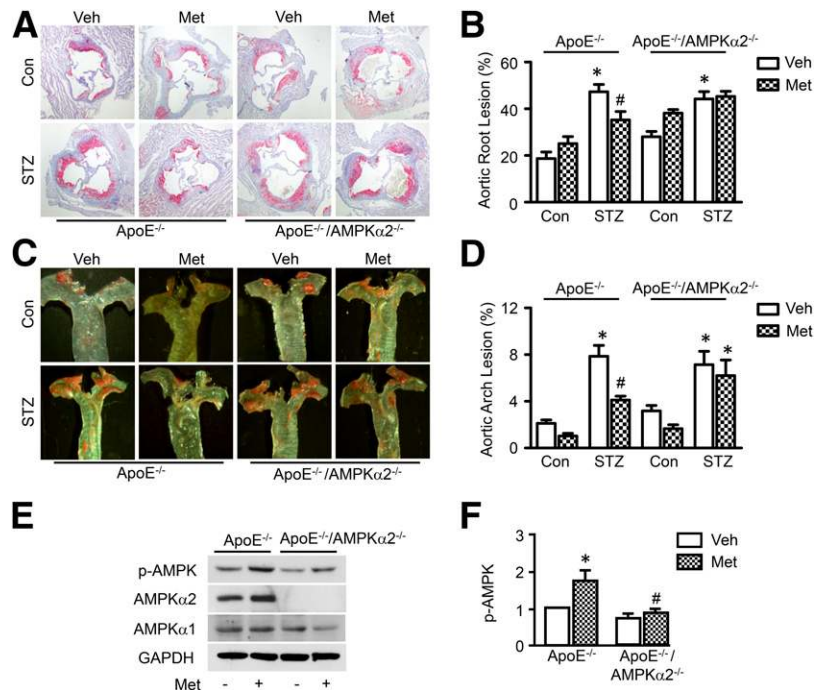


Figure 1—Metformin reduces atherosclerotic lesions in diabetic ApoE^{-/-} mice, but not in diabetic ApoE^{-/-}/AMPK-α2^{-/-} mice. ApoE^{-/-} and ApoE^{-/-}/AMPK-α2^{-/-} mice were induced with diabetes by STZ injection and treated with metformin (Met; 300 mg/kg/d) or vehicle (Veh) for 12 weeks ($n = 8-10$ per group). *A*: Representative images of Oil Red O staining of atherosclerotic lesions at the aortic sinus. *B*: Quantitative analysis of atherosclerotic lesion size in the aortic root. *C*: Representative images of Sudan IV staining of atherosclerotic lesions at the aortic arch. *D*: Quantitative analysis of the en face atherosclerotic lesion area in the aortic arch. * $P < 0.05$ vs. control mice (Con); # $P < 0.05$ vs. Veh. Phosphorylation of AMPK at Thr-172 (p-AMPK) (*E*) and expression of total AMPK-α1 and AMPK-α2 in the aorta (*F*) were determined by Western blotting. $n = 4$; * $P < 0.05$ vs. Veh; # $P < 0.05$ vs. WT.

diabetes-accelerated atherosclerosis in an AMPK-α2-dependent manner.

Metformin Inhibits Mitochondrial-Derived Superoxide Production and Oxidative Stress Under Diabetic Conditions

Mitochondria-derived superoxide anions serve as the major intracellular source of ROS in diabetes (33). Overproduction of ROS induces oxidative stress and organ damage, which is a risk factor for atherosclerosis and diabetic complications. We next determined whether metformin reduces atherosclerosis by inhibiting mitochondrial ROS production and oxidative damage in diabetes. We measured mitochondrial superoxide anion production in vivo by incubating freshly isolated aortas with fluoroprobe MitoSOX Red using high-performance liquid chromatography, which selectively targets to the mitochondria and exhibits red fluorescence when oxidized by mitochondrial superoxide. As expected, diabetic aortas exhibited higher levels of mitochondria-derived superoxide anions than control mouse aortas. Metformin treatment almost completely inhibited the overproduction of mitochondrial superoxide anions (Fig. 2A). In addition, DHE staining, which is extensively used to evaluate ROS production, verified that metformin significantly attenuated cellular ROS production in diabetic mouse aortas (Fig. 2B and C).

We next examined whether metformin inhibits diabetes-induced oxidative stress by detecting levels of 8-OHdG and 3-NT proteins in the aortas from the diabetic ApoE^{-/-} and ApoE^{-/-}/AMPK-α2^{-/-} mice. Levels of 8-OHdG, a biomarker for oxidative DNA damage, were markedly elevated in diabetic mouse aortas, especially in the aortic endothelium. Metformin treatment significantly reduced 8-OHdG levels in ApoE^{-/-} mice but not in ApoE^{-/-}/AMPK-α2^{-/-} mice (Fig. 2D and E). Similarly, levels of 3-NT, a marker of oxidative damage by protein tyrosine nitration, were increased in the aortas from diabetic ApoE^{-/-} mice. Metformin significantly abrogated the increase in 3-NT protein levels in the aortic endothelium of diabetic ApoE^{-/-} mice but not ApoE^{-/-}/AMPK-α2^{-/-} mice (Fig. 2F and G).

Metformin Prevents Hyperglycemia-Induced Mitochondrial Fragmentation

The disruption of mitochondrial dynamics and mitochondrial fragmentation increases mitochondrial ROS production in diabetes (7). To determine whether metformin inhibits mitochondrial ROS production by regulating mitochondrial dynamics, electron microscopy was used to observe mitochondrial morphology in the aortic endothelium. In the nondiabetic mouse aortic endothelium, mitochondria showed a long filamentous morphology with integrated double membranes and tight cristae. In contrast, most mitochondria became smaller and punctate

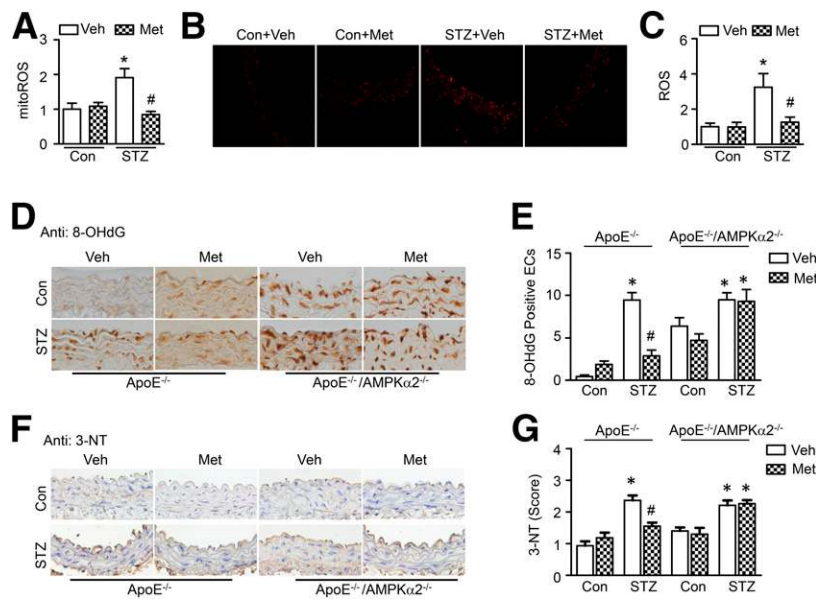


Figure 2—Metformin inhibits mitochondrial ROS (mitoROS) production and oxidative stress. **A–C:** STZ-induced diabetic C57BL/6J WT mice were treated with metformin (Met; 300 mg/kg/d) or vehicle (Veh) in drinking water for 4 weeks. **A:** Thoracic aortas were incubated in Krebs buffer with 2 $\mu\text{mol/L}$ MitoSOX Red for 30 min. Mitochondrial superoxide was measured by high-performance liquid chromatography ($n = 4$). **B:** Frozen thoracic aortic sections were incubated with 5 $\mu\text{mol/L}$ DHE for 30 min and analyzed using fluorescence microscopy. **C:** Quantification of fluorescence intensity for ROS levels in the aorta (original magnification $\times 40$). $n = 4$. * $P < 0.05$ vs. control (Con); # $P < 0.05$ vs. Veh. **D–G:** STZ-induced diabetic ApoE^{-/-} and ApoE^{-/-}/AMPK α 2^{-/-} mice were treated with metformin or vehicle for 12 weeks. **D:** Representative images of the immunohistochemical staining of 8-OHdG on thoracic aortic sections (original magnification $\times 40$). **E:** Quantification of 8-OHdG-positive endothelial cells (ECs). $n = 6$. * $P < 0.05$ vs. Con; # $P < 0.05$ vs. Veh. **F:** Representative images of the immunohistochemical staining of 3-NT (original magnification $\times 40$). **G:** Quantification of positive staining for 3-NT in thoracic aortic sections. $n = 5$. * $P < 0.05$ vs. Con; # $P < 0.05$ vs. Veh.

with significantly short in length in diabetic mouse aortic endothelial cells (Fig. 3A and B). These were suggestive of mitochondrial fragmentation. The mitochondrial fragmentation in diabetic mice was attenuated after correcting hyperglycemia to normoglycemia by insulin injection, indicating that hyperglycemia triggers mitochondrial fragmentation in diabetic mice. Moreover, administration of metformin reduced diabetes-induced mitochondrial fragmentation (Fig. 3A and B) and increased mitochondrial volume density (Supplementary Fig. 1), although it did not reduce blood glucose levels (vehicle vs. metformin: 434 ± 25 vs. 403 ± 20 mg/dL) in diabetic mice.

We then investigated whether metformin inhibits high glucose-induced mitochondrial fragmentation in HUVECs by visualizing mitochondrial morphology with MitoTracker Deep Red. In HUVECs cultured in normal glucose medium, mitochondria mainly appeared as elongated tubules with highly interconnecting networks. After stimulation with high glucose, mitochondria became spherical and shorter, and the number of mitochondria increased, indicating mitochondrial fragmentation. Mitochondrial morphology did not change in cells cultured in normal glucose or osmotic control medium. Notably, metformin treatment attenuated high glucose-induced mitochondrial fragmentation (Fig. 3C–E). Moreover, silencing AMPK- α 2 expression with small interfering (si)RNA blocks the inhibitory effect of metformin on mitochondrial fission in HUVECs

in response to high glucose (Fig. 3F–H and Supplementary Fig. 2).

Metformin Inhibits High Glucose-Induced Mitochondrial Fission by Reducing Drp-1 Expression

To gain insight into the mechanism by which metformin inhibits mitochondrial fragmentation, we assessed the expression of mitochondrial fission-related proteins, including Drp1 and Fis1, mitochondrial fusion-related proteins, including MFN2 and optic atrophy 1 (OPA1), and regulators of mitochondrial biogenesis, including peroxisome proliferator-activated receptor γ coactivator 1 α (PGC-1 α) and mitochondrial transcription factor A (mtTFA), in diabetic mouse aortas. Compared with nondiabetic mouse aortas, diabetic mouse aortas exhibited higher levels of Drp1. However, there were no significant differences in the protein levels of Fis1, MFN2, and OPA1 between diabetic and nondiabetic mice. Normalization of blood glucose by insulin injection mitigated diabetes-enhanced Drp1 expression, suggesting that hyperglycemia plays an essential role in the upregulation of Drp1 expression (Fig. 4A and Supplementary Fig. 4A). Furthermore, metformin treatment reduced hyperglycemia-enhanced Drp1 expression but had no effect on the expression of Fis1, MFN2, and OPA1 in mouse aortas (Fig. 4B and Supplementary Fig. 4B). Meanwhile, administration of metformin increased PGC-1 α and mtTFA protein expression in aortas from

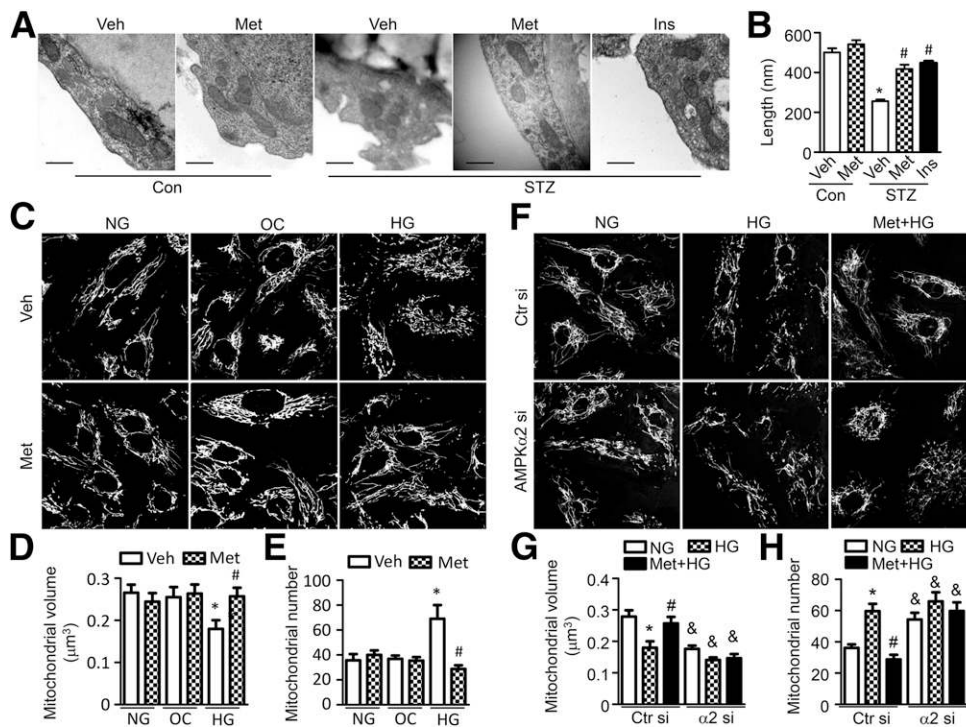


Figure 3—Metformin diminishes hyperglycemia-induced mitochondrial fragmentation in endothelial cells. *A* and *B*: STZ-induced diabetic WT mice were administrated with metformin (Met; 300 mg/kg/d) or vehicle (Veh) for 4 weeks or intraperitoneally injected with insulin (STZ+Ins, 0.5 units/kg, twice per day) for 14 days. *A*: Representative electron microscopic images of mitochondria in the aortic endothelium (original magnification $\times 25,000$; scale bar = 500 nm). *B*: Quantification of mitochondrial length. $n = 6$ mice, at least 50 mitochondria per mice were analyzed. $*P < 0.05$ vs. control (Con); $\#P < 0.05$ vs. Veh. *C–E*: HUVECs were pretreated with 2 mmol/L metformin for 2 h and cultured in EB medium containing normal glucose (NG), 30 mmol/L D-glucose (high glucose [HG]), or 25 mmol/L mannitol plus 5 mmol/L D-glucose (osmotic control [OC]) for 24 h. *F–H*: HUVECs were transfected with control siRNA (Ctr si) or AMPK- $\alpha 2$ siRNA ($\alpha 2$ si) for 48 h, then pretreated with 2 mmol/L metformin for 2 h and cultured with high-glucose medium for 24 h. Mitochondria were labeled with MitoTracker Deep Red, and mitochondrial morphology was analyzed using fluorescence microscopy. Mitochondrial volume and number were quantified, as described in the RESEARCH DESIGN AND METHODS. $n \geq 100$. $*P < 0.05$ vs. NG; $\#P < 0.05$ vs. Veh; $\&P < 0.05$ vs. Ctr si.

both nondiabetic and diabetic mice (Supplementary Fig. 3). Next, we detected Drp1 expression in aortas from diabetic ApoE^{-/-} and ApoE^{-/-}/AMPK- $\alpha 2$ ^{-/-} mice by immunohistochemistry. Diabetes increased Drp1 expression in the ApoE^{-/-} aortic endothelium and induced a further increase in Drp1 expression in the ApoE^{-/-}/AMPK- $\alpha 2$ ^{-/-} aortic endothelium. Metformin treatment reduced Drp1 expression in the aortic endothelium of diabetic ApoE^{-/-} mice but did not affect Drp1 expression in the aortic endothelium of diabetic ApoE^{-/-}/AMPK- $\alpha 2$ ^{-/-} mice (Fig. 4C and Supplementary Fig. 4C).

We also investigated the effect of metformin on Drp1 expression in cultured HUVECs. Compared with normal glucose and osmotic control treatments, high glucose increased Drp1 expression without affecting Fis1, MFN2, and OPA1 expression (Fig. 4D and Supplementary Fig. 4D). To study whether Mff participates in regulating mitochondrial dynamics in endothelial cells, we detected its expression in HUVECs, human VSMCs (HVSMCs), HeLa cells, and human lung cancer cells (H1299). Large amounts of Mff were expressed in HeLa and H1299 cells but not in HUVECs and HVSMCs (Fig. 4E and Supplementary Fig. 4E). Metformin treatment reduced Drp1 protein

levels in total lysates (Fig. 4F and Supplementary Fig. 4F), cytoplasmic fractions, and mitochondrial fractions (Fig. 4G and Supplementary Fig. 4G). We further examined whether metformin regulates mitochondrial dynamics by using time-lapse confocal imaging to evaluate the occurrence of mitochondrial fission in live HUVECs. Mitochondrial fission occurred at a higher frequency after high glucose stimulation than after normal glucose treatment (17 ± 2 vs. 32 ± 3 events/cell in 10 min). Importantly, metformin inhibited high glucose-induced mitochondrial fission (Fig. 4H and I).

AMPK Activation Reduces Drp1 Expression and Mitochondrial Fragmentation

We further tested whether AMPK activation is required for the metformin-induced inhibition of mitochondrial fission. Diabetes inhibited AMPK phosphorylation and acetyl-CoA carboxylase (ACC) phosphorylation in mouse aortas, and the reduction in phosphorylation was prevented by metformin treatment (Fig. 5A). Similar results were observed in cultured HUVECs (Fig. 5B). To verify these results using a genetic approach, we transfected HUVECs with an adenovirus encoding the constitutively

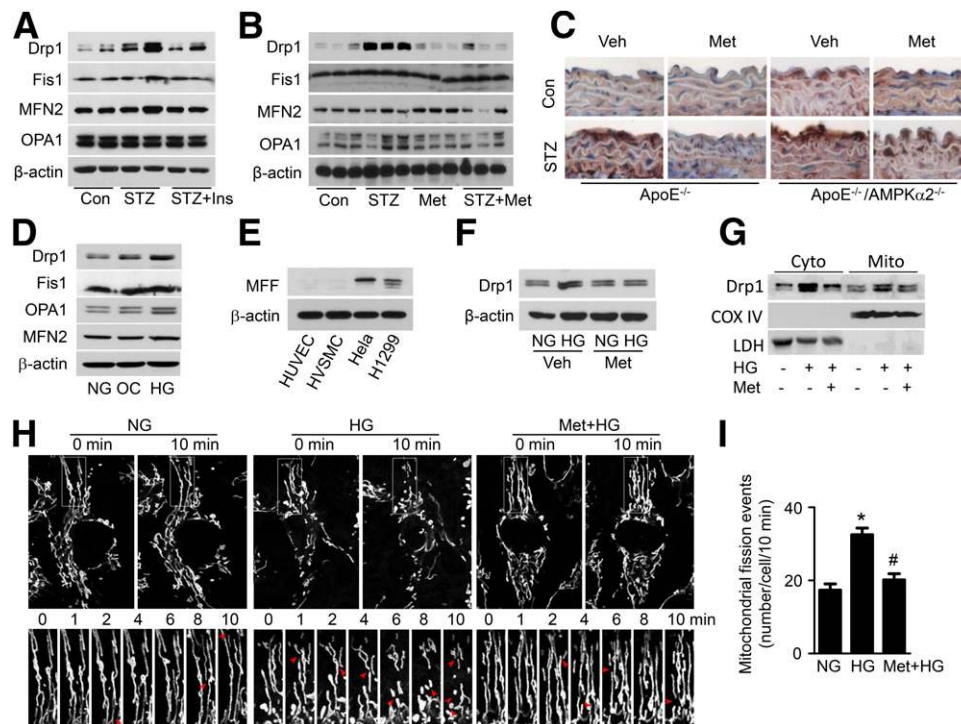


Figure 4—Metformin downregulates Drp1 expression and mitochondrial fission. STZ-induced diabetic WT mice were intraperitoneally injected with 0.5 units/kg insulin (Ins) for 14 days (A) or administered metformin (Met; 300 mg/kg/d) in drinking water for 4 weeks (B). Mitochondrial dynamics-related proteins, including Drp1, mitochondrial Fis1 protein, MFN2, and OPA1, in the aorta were analyzed by Western blotting. C: Representative of immunohistochemical staining of Drp1 on thoracic aortic sections from diabetic ApoE^{-/-} and ApoE^{-/-}/AMPK- α 2^{-/-} mice treated with metformin. D: HUVECs were treated with normal glucose (NG), 30 mmol/L D-glucose (high glucose [HG]), or 25 mmol/L mannitol plus 5 mmol/L D-glucose (osmotic control [OC]) for 24 h. Mitochondrial Drp1 protein expression was determined by Western blotting. E: Protein levels of mitochondrial MFF in HUVECs, HVSMCs, HeLa cells, and H1299 cells. F–I: HUVECs were pretreated with 2 mmol/L metformin for 2 h, followed by stimulation with high glucose for 24 h. F: Drp1 protein level was measured by Western blotting. G: Western blot analysis of Drp1 protein levels in cytoplasmic (Cyto) and mitochondrial (Mito) fractions. Cyclooxygenase (COX) IV and lactate dehydrogenase (LDH) were used as mitochondrial and cytosolic markers, respectively. H: Mitochondrial morphology in live HUVECs stained with MitoTracker Deep Red FM was captured using time-lapse confocal microscopy. Images were collected at 1-min intervals for 10 min. I: Quantification of mitochondrial fission events in live HUVECs. $n = 15$. * $P < 0.05$ vs. NG; # $P < 0.05$ vs. HG. Veh, vehicle.

active form of AMPK (AMPK-CA), which increased the phosphorylation of AMPK and ACC (Fig. 5C). Transfection with the AMPK-CA adenovirus also reduced Drp1 protein expression and mitochondrial fragmentation in high glucose-treated HUVECs (Fig. 5D–F). To investigate whether Drp1 is required for mitochondrial fission in high glucose-treated endothelial cells, we transfected HUVECs with Drp1 siRNA. Drp1 siRNA transfection significantly reduced Drp1 protein expression in normal glucose- and high glucose-treated HUVECs (Fig. 5G) and reduced mitochondrial fragmentation in high glucose-treated HUVECs (Fig. 5H–J). Overall, these data suggest that metformin prevents mitochondrial fragmentation via the AMPK-dependent downregulation of Drp1 protein expression.

Inhibition of Drp1 Attenuates Oxidative Stress in Diabetes

Metformin inhibited Drp1-mediated mitochondrial fission and mitochondrial ROS production in diabetes; however, whether increased mitochondrial fission causes oxidative stress remains unclear. We therefore used the

Drp1 inhibitor, mdivi-1, and Drp1 siRNA to investigate whether the inhibition of Drp1-mediated mitochondrial fission reduces oxidative stress in vivo and in vitro. Administration of mdivi-1 significantly attenuated mitochondrial fragmentation in aortic endothelial cells from diabetic mice (Fig. 6A and B) and did not affect body weight (mdivi-1 vs. DMSO: 20.4 \pm 0.5 g vs. 20.7 \pm 1.0 g) and blood glucose (mdivi-1 vs. DMSO: 436 \pm 21 mg/dL vs. 444 \pm 24 mg/dL). In addition, mdivi-1 markedly attenuated ROS production (Fig. 6C) and reduced levels of 3-NT (Fig. 6D) and 8-OHdG (Fig. 6E) in aortas from diabetic mice. Gene silencing of Drp1 consistently reduced mitochondrial-derived superoxide production in high glucose-treated HUVECs (Fig. 6F and G).

Metformin and Mdivi-1 Prevent Endothelial Dysfunction and Inflammation in Diabetes

Abnormal superoxide anion reduces NO bioavailability and converts NO into peroxynitrite, which causes endothelial dysfunction and endothelial inflammation, thereby contributing to the development of atherosclerosis (34). We first assessed Ach-mediated vasodilation in aortic

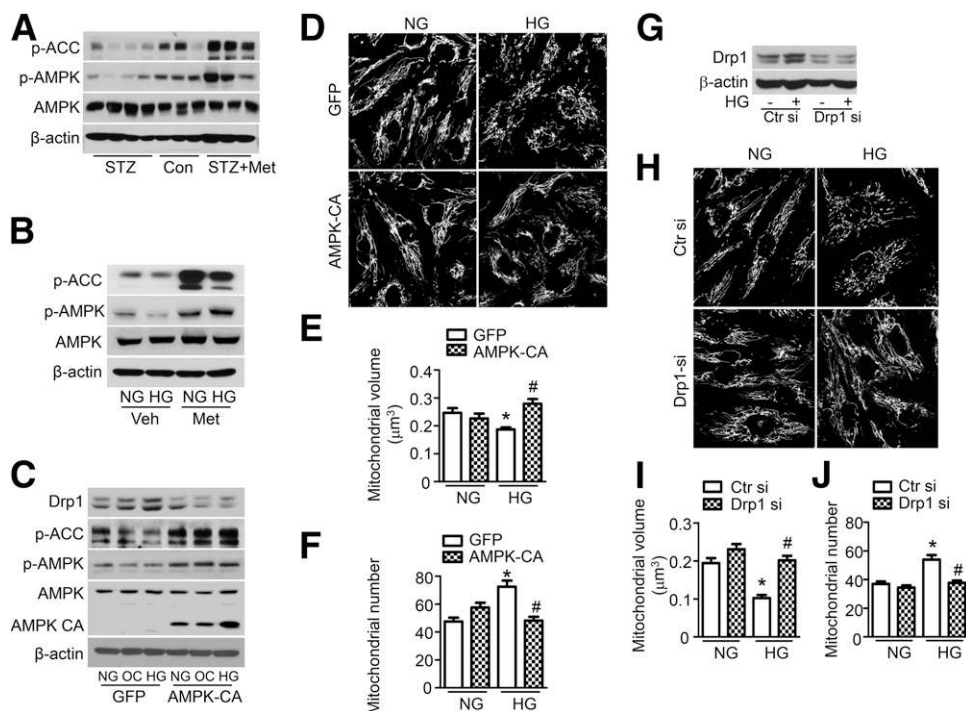


Figure 5—AMPK activation inhibits Drp1-mediated mitochondrial fission. **A**: STZ-induced diabetic WT mice were treated with metformin (Met; 300 mg/kg/d) for 4 weeks. Phosphorylation of AMPK (p-AMPK) at Thr-172 and phosphorylation of ACC (p-ACC) at Ser-79 in the aorta were measured by Western blotting. **B**: HUVECs were pretreated with 2 mmol/L metformin for 2 h and then treated with normal glucose (NG) or high glucose (HG) for 24 h. Phosphorylation of AMPK and ACC was measured by Western blotting. **C–F**: HUVECs were transfected with adenovirus (Ad)-AMPK-CA or Ad-GFP for 24 h, after which they were treated with high glucose for 24 h. **C**: Drp1 expression, p-AMPK, and p-ACC were measured by Western blotting. **D**: Representative images of mitochondrial morphology were captured at original magnification $\times 40$. Mitochondrial volume (**E**) and number (**F**) were analyzed, as described in the RESEARCH DESIGN AND METHODS. $n \geq 100$. * $P < 0.05$ vs. NG; # $P < 0.05$ vs. GFP. **G–J**: HUVECs were transfected with Drp1 siRNA (si) for 48 h and then stimulated with high glucose for 24 h. **G**: Drp1 expression was measured by Western blotting. **H**: Representative images of mitochondrial morphology were captured at original magnification $\times 40$. Mitochondrial volume (**I**) and number (**J**) were analyzed as described in the RESEARCH DESIGN AND METHODS. $n \geq 100$. * $P < 0.05$ vs. NG; # $P < 0.05$ vs. control siRNA. OC, osmotic control; Veh, vehicle.

rings from STZ-induced diabetic mice treated with mdivi-1. Compared with control aortic rings, diabetic aortic rings exhibited an impairment in Ach-induced, endothelium-dependent relaxation. Mdivi-1 treatment significantly attenuated the impairment (Fig. 7A) without affecting SNP-induced, endothelium-independent vasodilator responses (Fig. 7B). This suggests that inhibition of mitochondrial fission protects against endothelial dysfunction in diabetes. Metformin treatment consistently attenuated the impairment of Ach-induced relaxation without affecting SNP-induced relaxation in diabetic mice (Fig. 7C and D).

The expression of ICAM-1 and VCAM-1 was higher in the aortic endothelium from diabetic mice than nondiabetic control mice. Mdivi-1 treatment attenuated diabetes-enhanced ICAM-1 and VCAM-1 expression in the aortic endothelium (Fig. 7E and F). Moreover, metformin significantly abrogated the increase in ICAM-1 and VCAM-1 levels in the aortic endothelium of diabetic ApoE^{-/-} mice but not ApoE^{-/-}/AMPK- $\alpha 2$ ^{-/-} mice (Fig. 7G and H). More importantly, immunofluorescence staining showed that metformin reduced the expression of ICAM-1 and VCAM-1

in aortic atherosclerotic lesions from diabetic ApoE^{-/-} mice but not in lesions from diabetic ApoE^{-/-}/AMPK- $\alpha 2$ ^{-/-} mice (Fig. 7I and J). This supports the concept that metformin prevents mitochondrial fragmentation and endothelial inflammation in an AMPK-dependent manner.

Inhibition of Mitochondrial Fission Reduces Atherosclerotic Lesions in Diabetes

Finally, we assessed the relationship between increased mitochondrial fission and the progression of atherosclerosis in diabetic ApoE^{-/-} mice intraperitoneally treated with mdivi-1 (10 mg/kg twice per week, 8 weeks). Compared with nondiabetic ApoE^{-/-} mice, diabetic ApoE^{-/-} mice had more atherosclerotic lesions. Most importantly, mdivi-1 treatment significantly reduced the severity of atherosclerotic lesions in the aortic root and aortic arch in diabetic ApoE^{-/-} mice, but not in nondiabetic ApoE^{-/-} mice (Fig. 8A–D). Moreover, mdivi-1 did not significantly change blood glucose, serum cholesterol, and serum triglyceride levels in diabetic ApoE^{-/-} mice (Supplementary Table 3).

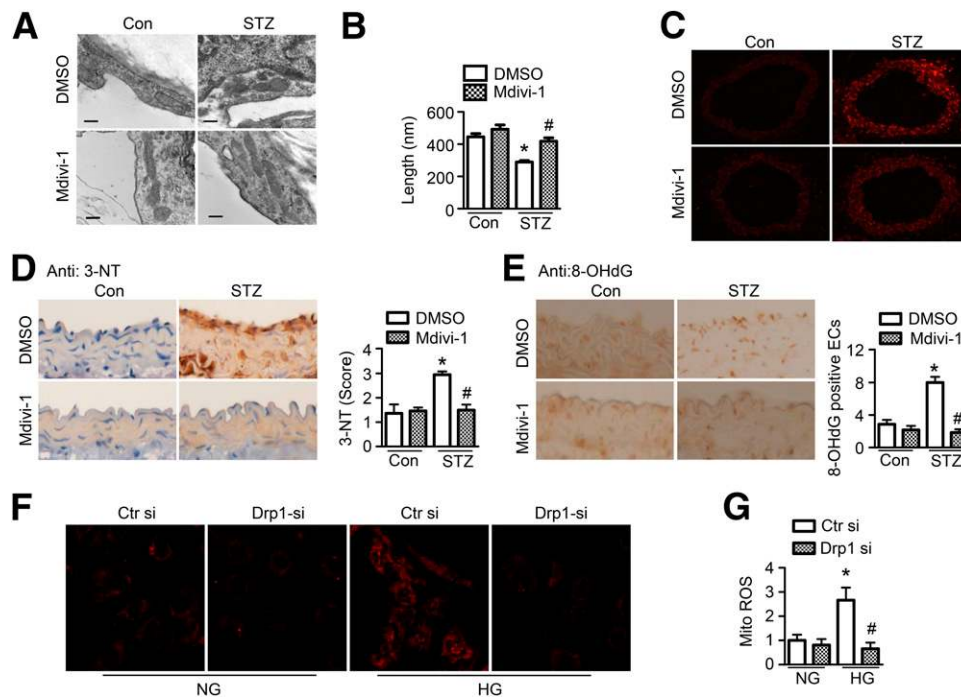


Figure 6—Inhibition of mitochondrial fission attenuates oxidative stress in diabetic aorta. *A–F*: STZ-induced diabetic mice were treated with mdivi-1 (1.2 mg/kg/d) or vehicle (DMSO) using an osmotic pump for 14 days. *A*: Representative transmission electron micrographs of mitochondria in the aortic endothelium. Scale bars = 300 nm. *B*: Quantification of average mitochondrial length. $n = 6$ mice, at least 50 mitochondria per mice were analyzed. * $P < 0.05$ vs. control mice; # $P < 0.05$ vs. DMSO. *C*: Frozen sections of aortas were incubated with 5 $\mu\text{mol/L}$ DHE for 30 min. Images were obtained at 518 nm (excitation) and 605 nm (emission). $n = 5$. *D*: Representative images of immunohistochemical staining and quantification of positive staining for 3-NT in thoracic aortic sections. $n = 5$. * $P < 0.05$ vs. control; # $P < 0.05$ vs. vehicle. *E*: Representative images of immunohistochemical staining for 8-OHdG in aortas. Quantification of 8-OHdG-positive endothelial cells (ECs). $n = 5$ mice. * $P < 0.05$ vs. control mice; # $P < 0.05$ vs. DMSO. *F* and *G*: HUVECs were transfected with Drp1 siRNA (si) or control siRNA for 24 h, after which they were treated with high glucose (HG) for 24 h. Mitochondrial ROS production was measured by incubating HUVECs with 2 $\mu\text{mol/L}$ MitoSOX for 30 min. *F*: Representative fluorescence images are shown. *G*: Quantification of fluorescence intensity for mitochondrial ROS levels in HUVECs. $n = 6$. * $P < 0.05$ vs. normal glucose (NG); # $P < 0.05$ vs. control siRNA.

DISCUSSION

In this study, we uncover a novel mechanism by which metformin inhibits the development of atherosclerosis in diabetes. Using STZ-induced diabetic ApoE^{-/-} mice, we demonstrate that metformin reduced Drp1 expression and Drp1-mediated mitochondrial fission in diabetic endothelial cells via an AMPK-dependent manner. The suppression of mitochondrial fission resulted in the inhibition of endothelial oxidative stress, improvement of endothelial function, and reduction in atherosclerotic lesions. In addition, administration of mdivi-1, a mitochondrial fission inhibitor, protected against atherosclerosis, reduced mitochondrial ROS production, inhibited vascular inflammation, and improved endothelial function. Our data demonstrate that metformin prevents the development of atherosclerosis by inhibiting Drp1-dependent mitochondrial fission.

Mitochondria are highly dynamic organelles that are intimately involved in various cellular functions, including energy metabolism, ROS production, stress response, and cell death (35,36). Accumulating evidence suggests that mitochondrial oxidative damage has a causative role in the pathogenesis of atherosclerosis. For instance, dysfunction in

the mitochondrial ETC complex increases mitochondrial oxidative stress and promotes the development of atherosclerosis in paraoxonase2^{-/-}/ApoE^{-/-} mice (37). Conversely, overexpression of the mitochondrial thioredoxin gene inhibits mitochondrial oxidative stress and reduces atherosclerotic lesion formation in ApoE^{-/-} mice (4). In diabetes, hyperglycemia is well documented to disrupt the balance between mitochondrial fusion and fission, leading to an increase in smaller individual mitochondrion (9) that are prone to producing excessive ROS. In the current study, we provide compelling evidence showing that increased Drp1 protein and mitochondrial fragmentations occurred in aortic endothelial cells during diabetes-accelerated atherosclerosis. Administration of the Drp1 inhibitor, mdivi-1, dramatically reduced atherosclerotic lesion formation in STZ-induced diabetic ApoE^{-/-} mice. Meanwhile, mdivi-1 suppressed mitochondrial ROS production and cellular oxidative stress. Therefore, our results suggest that increased mitochondrial fragmentation may accelerate atherosclerosis in diabetes. Overall, our study develops a new concept that mitochondrial fission contributes to atherogenesis in diabetes, partly by enhancing mitochondrial oxidative stress.

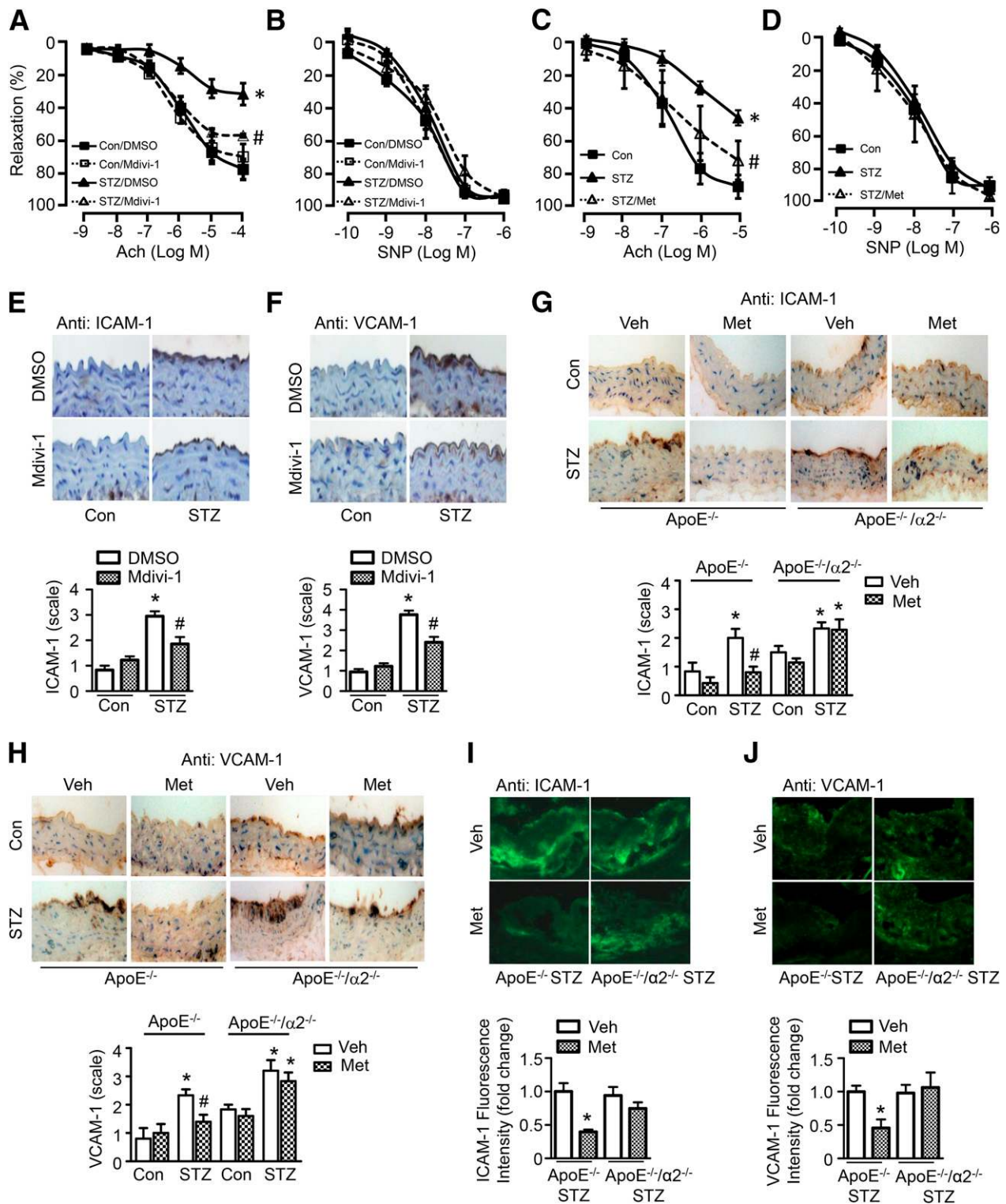


Figure 7—Inhibition of mitochondrial fission attenuates endothelial dysfunction in diabetic mice. **A** and **B**: STZ-induced diabetic mice were treated with mdivi-1 (1.2 mg/kg/d) or vehicle (DMSO) for 14 days. **C** and **D**: STZ-induced diabetic mice were treated with metformin (Met; 300 mg/kg/d) for 4 weeks. Aortic rings were contracted with U46619 (30 nmol/L). Endothelium-dependent vasodilator responses were measured in the presence of ACh (10^{-9} to 10^{-5} mol/L). Endothelium-independent vasodilator responses were measured in the presence of SNP (10^{-10} to 10^{-6} mol/L). $n = 6-8$. * $P < 0.05$ vs. control; # $P < 0.05$ vs. STZ. Immunohistochemical staining for ICAM-1 (**E**) and VCAM-1 (**F**) in aortas from mdivi-1-treated diabetic mice. **G** and **H**: Immunohistochemical staining and quantification of positive staining for ICAM-1 and VCAM-1 in aortas from diabetic ApoE^{-/-} and ApoE^{-/-}/AMPK- α 2^{-/-} mice treated with metformin or vehicle (Veh). $n = 5$; * $P < 0.05$ vs. control, # $P < 0.05$ vs. Veh. **I** and **J**: Immunofluorescence staining for ICAM-1 and VCAM-1 in atherosclerotic lesions of diabetic ApoE^{-/-} and ApoE^{-/-}/AMPK- α 2^{-/-} mice treated with metformin or vehicle. $n = 4$. * $P < 0.05$ vs. Veh.

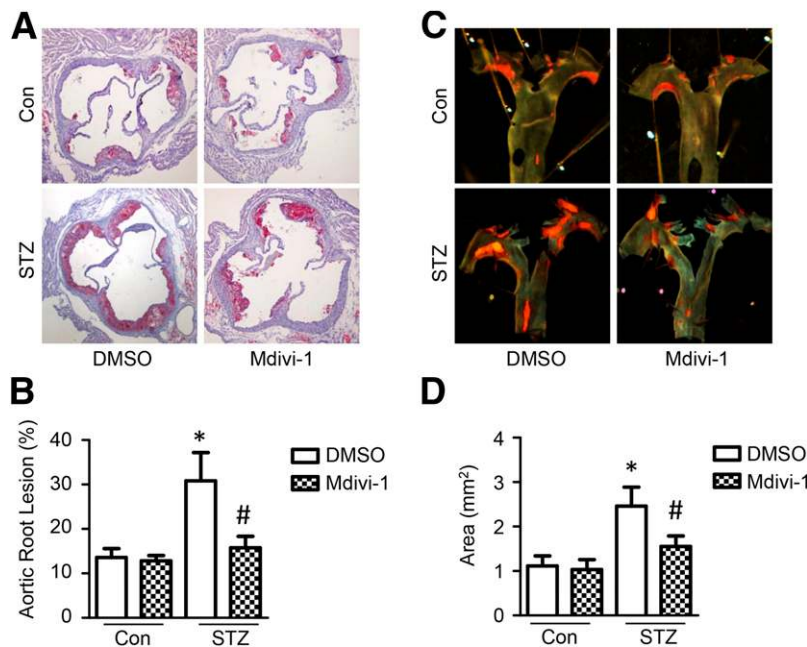


Figure 8—Inhibition of mitochondrial fission attenuates hyperglycemia-accelerated atherosclerosis. ApoE^{-/-} mice were induced with diabetes by STZ injection and treated with mdivi-1 (10 mg/kg, twice per week) or vehicle (DMSO) for 8 weeks. *A*: Representative images of Oil Red O staining of atherosclerotic lesions at the aortic sinus. *B*: Quantitative analysis of atherosclerotic lesion size in the aortic root. *C*: Representative images of Sudan IV staining of atherosclerotic lesions at the aortic arch. *D*: Quantitative analysis of en face atherosclerotic lesion areas in the aortic arch. *n* = 10. **P* < 0.05 vs. control; #*P* < 0.05 vs. DMSO.

Another group also showed that metformin prevents ROS-mediated mitochondrial fission via AMPK activation in HUVECs (15). To support this conclusion, we found that the activation of AMPK by metformin reduced Drp1 expression and mitochondrial fragmentations in diabetic aortic endothelial cells. Similar to the antiatherosclerotic effect of mdivi-1, metformin inhibits accelerated atherosclerotic lesion formation in diabetic ApoE^{-/-} mice. However, metformin could not reduce the hyperglycemia-accelerated development of atherosclerosis in ApoE^{-/-}/AMPK- α 2^{-/-} mice, suggesting that its antiatherosclerotic effect may be attributed to the action of AMPK on mitochondrial dynamics. However, the effects of metformin on mitochondria activities might be multiple, well beyond its regulation on mitochondrial dynamics. For example, we found that metformin enhanced the expression of PGC-1 α and mtTFA protein, the regulators of mitochondrial biogenesis. Similarly, Nishikawa and colleagues (38,39) demonstrated that AMPK activation by metformin and thiazolidinediones promotes mitochondrial biogenesis and reduces hyperglycemia-induced mitochondrial ROS production in cultured endothelial cells. Therefore, mitochondrial dynamics and mitochondrial biogenesis might both be potential contributors in the metformin-mediated mitochondrial adaptations. In addition, metformin attenuates the high-fat diet- or angiotensin II-induced formation of atheromatous plaques by downregulating the angiotensin II receptor and reducing monocyte-to-macrophage differentiation (40,41). Clinical trials have demonstrated that metformin reduces cardiovascular complications, including atherosclerosis and

myocardial infarction, in patients with diabetes. The UK Prospective Diabetes study reported that metformin administration significantly reduced the progression of common carotid intima-media thickness in patients with T2DM (17). Zhang et al. (18) further confirmed the antiatherosclerotic effect of metformin in 140 patients with T2DM in China. The present work indicates that metformin-inhibited mitochondrial fission may be a novel mechanism underlying its antiatherosclerotic effect in diabetes.

Drp1 is a cytosolic guanosine-5'-triphosphate-hydrolyzing mechanoenzyme that triggers mitochondrial division by binding to Fis1 or Mff on mitochondria in mammalian cells. The regulation of Drp1 properties, such as protein expression, mitochondrial translocation, and posttranscriptional modification, might be important for the modulation of Drp1 function. Previous studies have shown that high glucose increases Drp1 protein expression in endothelial cells, glomerular mesangial cells (42), hippocampal neurons (43), and pancreatic β -cells (44). In this study, we demonstrate that the activation of AMPK by metformin reduced Drp1 expression and inhibited Drp1-mediated mitochondrial fission. Consistently, metformin has been shown to inhibit mitochondrial fission and reduce endothelial cell apoptosis via the downregulation of Drp1 expression in high glucose-stimulated endothelial cells (15). Furthermore, overexpression of constitutively active AMPK reduced Drp1 expression and mitochondrial fragmentations. In contrast, AMPK- α 2 deficiency blocks the inhibitory effect of metformin on mitochondrial fission in response to high glucose,

suggesting that AMPK- α 2 is required for the inhibitory effect of metformin on mitochondrial fission. Interesting, AMPK- α 1 is the major isoform in endothelial cells (45); however, AMPK- α 1 and AMPK- α 2 are both essential in maintaining endothelial function. For example, activation of AMPK- α 1 or AMPK- α 2 can improve endothelial function via directly phosphorylating eNOS at Ser1177 and Ser635 (46,47). Therefore, whether AMPK- α 1 is involved in these processes requires additional investigation. AMPK is a well-known autophagy activator that can activate the mammalian target of rapamycin and Unc-51-like autophagy activating kinase 1 pathways (48). Our laboratory and others have identified that Drp1 can be degraded via the autophagy-lysosome pathway (49). It is possible that metformin may reduce Drp1 expression by enhancing the autophagy-dependent degradation of Drp1. In addition to regulating Drp1 protein expression, AMPK directly phosphorylates Drp1 at Ser-637, thus inhibiting Drp1 activity and preventing its translocation to mitochondria in diabetic mouse adipose tissues and in palmitate-induced INS-1E β -cells (19,21). In the current study, metformin reduced Drp1 protein levels in both cytoplasmic and mitochondrial fractions, suggesting that metformin regulates mitochondrial fission by reducing Drp1 expression and inhibiting its activity. Toyama et al. (50) recently reported that AICAR induces mitochondrial fission by phosphorylating Mff at Ser-172 in human U2OS osteosarcoma cells. In the current study, Mff was rarely expressed in HUVECs and HVSMCs. Consistently, the Human Protein Atlas Program reported a very low expression of Mff protein in endothelial cells in human colon and cerebral cortex tissues (<http://www.proteinatlas.org/ENSG00000168958-MFF/tissue/primary+data>). These results partially explain the controversial effects of AMPK activation on mitochondrial dynamics in endothelial cells and cancer cells.

The increased production of ROS is a key event in the pathogenesis of endothelial dysfunction, because ROS reduces NO bioavailability by reacting with NO to form peroxynitrite. In the current study, inhibition of mitochondrial fission by mdivi-1 or metformin improved endothelium-dependent relaxation. Similarly, Drp1 siRNA enhances NO bioavailability and cyclic guanosine monophosphate production in venous endothelial cells isolated from patients with diabetes (9). These results suggest that the enhancement in mitochondrial fission increases ROS production and impairs endothelial function. Moreover, pharmacological activation of AMPK by metformin, salicylate, and AICAR reduces mitochondrial fission, accompanied by enhanced eNOS phosphorylation and improved endothelium-dependent vasodilation (20). Emerging evidence indicates that other redox pathways, such as NADPH oxidases (Nox) and eNOS uncoupling, are involved in endothelial dysfunction and the development of atherosclerosis in diabetes. Genetic deletion and pharmacological inhibition of Nox1 decreases atherosclerotic lesion formation in STZ-injected diabetic ApoE^{-/-} mice (51). In addition,

eNOS activation protects against diabetes-accelerated atherosclerosis in STZ-injected diabetic ApoE^{-/-} mice (52). Therefore, whether enhanced mitochondrial fission triggers other ROS sources, such as Nox1, Nox2, Nox4, and eNOS uncoupling, requires further examination.

The current study has some limitations. First, our experiments were exclusively done in STZ-made insulin-deficient type 1 diabetic mice. Whether the present findings can be applied to insulin-resistance T2DM warrants further investigation. The second limitation is that all experiments were done in global AMPK- α 2^{-/-} mice. The effects of endothelial cell-specific AMPK- α 2 or AMPK- α 2 deletion will be very useful in defining the relative contributions of endothelial cell AMPK- α 1 or AMPK- α 2 to atherosclerosis.

In conclusion, diabetes accelerated atherosclerosis by triggering Drp1-mediated mitochondrial fission. Activation of AMPK by metformin reduced Drp1 expression, mitochondrial fragmentation, and atherosclerotic lesions in diabetes. These findings identified mitochondrial fission as a target for treating atherosclerosis and other vascular disorders in diabetes.

Funding. This study was supported by National Heart, Lung, and Blood Institute grants HL-128014 and HL-132500 to Z.X. and M.-H.Z. and grants HL-079584, HL-080499, HL-089920, and HL-110488 to M.-H.Z. and National Institute on Aging grant AG-047776 to M.-H.Z.

Duality of Interest. No potential conflicts of interest relevant to this article were reported.

Author Contributions. Q.W. and M.Z. contributed to the design, researched data, and wrote the manuscript. G.T., C.O., and S.W. collected and analyzed data. Z.X. reviewed and edited the manuscript. M.-H.Z. contributed to the design, researched data, and wrote the manuscript. M.-H.Z. is the guarantor of this work and, as such, had full access to all the data in the study and takes responsibility for the integrity of the data and the accuracy of the data analysis.

References

- Prasad K, Dhar I. Oxidative stress as a mechanism of added sugar-induced cardiovascular disease. *Int J Angiol* 2014;23:217–226
- Song P, Zou MH. Redox regulation of endothelial cell fate. *Cell Mol Life Sci* 2014;71:3219–3239
- Brownlee M. Biochemistry and molecular cell biology of diabetic complications. *Nature* 2001;414:813–820
- Zhang H, Luo Y, Zhang W, et al. Endothelial-specific expression of mitochondrial thioredoxin improves endothelial cell function and reduces atherosclerotic lesions. *Am J Pathol* 2007;170:1108–1120
- Mercer JR, Yu E, Figg N, et al. The mitochondria-targeted antioxidant MitoQ decreases features of the metabolic syndrome in ATM^{+/-}/ApoE^{-/-} mice. *Free Radic Biol Med* 2012;52:841–849
- Westermann B. Mitochondrial fusion and fission in cell life and death. *Nat Rev Mol Cell Biol* 2010;11:872–884
- Yu T, Robotham JL, Yoon Y. Increased production of reactive oxygen species in hyperglycemic conditions requires dynamic change of mitochondrial morphology. *Proc Natl Acad Sci U S A* 2006;103:2653–2658
- Jheng HF, Tsai PJ, Guo SM, et al. Mitochondrial fission contributes to mitochondrial dysfunction and insulin resistance in skeletal muscle. *Mol Cell Biol* 2012;32:309–319
- Shenouda SM, Widlansky ME, Chen K, et al. Altered mitochondrial dynamics contributes to endothelial dysfunction in diabetes mellitus. *Circulation* 2011;124:444–453

10. Lugas JJ, Ngho GA, Bachschmid MM, Walsh K. Mitofusins are required for angiogenic function and modulate different signaling pathways in cultured endothelial cells. *J Mol Cell Cardiol* 2011;51:885–893
11. Wang W, Wang Y, Long J, et al. Mitochondrial fission triggered by hyperglycemia is mediated by ROCK1 activation in podocytes and endothelial cells. *Cell Metab* 2012;15:186–200
12. Westermeier F, Navarro-Marquez M, López-Crisosto C, et al. Defective insulin signaling and mitochondrial dynamics in diabetic cardiomyopathy. *Biochim Biophys Acta* 2015;1853:1113–1118
13. Zhan M, Usman IM, Sun L, Kanwar YS. Disruption of renal tubular mitochondrial quality control by Myo-inositol oxygenase in diabetic kidney disease. *J Am Soc Nephrol* 2015;26:1304–1321
14. Sajic M. Mitochondrial dynamics in peripheral neuropathies. *Antioxid Redox Signal* 2014;21:601–620
15. Bhatt MP, Lim YC, Kim YM, Ha KS. C-peptide activates AMPK α and prevents ROS-mediated mitochondrial fission and endothelial apoptosis in diabetes. *Diabetes* 2013;62:3851–3862
16. Hong J, Zhang Y, Lai S, et al.; SPREAD-DIMCAD Investigators. Effects of metformin versus glipizide on cardiovascular outcomes in patients with type 2 diabetes and coronary artery disease. *Diabetes Care* 2013;36:1304–1311
17. Matsumoto K, Sera Y, Abe Y, Tominaga T, Yeki Y, Miyake S. Metformin attenuates progression of carotid arterial wall thickness in patients with type 2 diabetes. *Diabetes Res Clin Pract* 2004;64:225–228
18. Zhang XY, Du JL, Jia YJ, et al. [Primary preventive effect of metformin upon atherosclerosis in patients with type 2 diabetes mellitus]. *Zhonghua Yi Xue Za Zhi* 2009;89:2134–2137
19. Li A, Zhang S, Li J, Liu K, Huang F, Liu B. Metformin and resveratrol inhibit Drp1-mediated mitochondrial fission and prevent ER stress-associated NLRP3 inflammasome activation in the adipose tissue of diabetic mice. *Mol Cell Endocrinol* 2016;434:36–47
20. Li J, Wang Y, Wang Y, et al. Pharmacological activation of AMPK prevents Drp1-mediated mitochondrial fission and alleviates endoplasmic reticulum stress-associated endothelial dysfunction. *J Mol Cell Cardiol* 2015;86:62–74
21. Wikstrom JD, Israeli T, Bachar-Wikstrom E, et al. AMPK regulates ER morphology and function in stressed pancreatic β -cells via phosphorylation of DRP1. *Mol Endocrinol* 2013;27:1706–1723
22. Morigi M, Perico L, Rota C, et al. Sirtuin 3-dependent mitochondrial dynamic improvements protect against acute kidney injury. *J Clin Invest* 2015;125:715–726
23. Sun R, Wang X, Liu Y, Xia M. Dietary supplementation with fish oil alters the expression levels of proteins governing mitochondrial dynamics and prevents high-fat diet-induced endothelial dysfunction. *Br J Nutr* 2014;112:145–153
24. Chen KH, Guo X, Ma D, et al. Dysregulation of HSG triggers vascular proliferative disorders. *Nat Cell Biol* 2004;6:872–883
25. Wang S, Zhang M, Liang B, et al. AMPK α 2 deletion causes aberrant expression and activation of NAD(P)H oxidase and consequent endothelial dysfunction in vivo: role of 26S proteasomes. *Circ Res* 2010;106:1117–1128
26. Dong Y, Zhang M, Liang B, et al. Reduction of AMP-activated protein kinase α 2 increases endoplasmic reticulum stress and atherosclerosis in vivo. *Circulation* 2010;121:792–803
27. Wang Q, Zhang M, Ding Y, et al. Activation of NAD(P)H oxidase by tryptophan-derived 3-hydroxykynurenine accelerates endothelial apoptosis and dysfunction in vivo. *Circ Res* 2014;114:480–492
28. Wang S, Xu J, Song P, Viollet B, Zou MH. In vivo activation of AMP-activated protein kinase attenuates diabetes-enhanced degradation of GTP cyclohydrolase I. *Diabetes* 2009;58:1893–1901
29. Zhang W, Wang Q, Wu Y, et al. Endothelial cell-specific liver kinase B1 deletion causes endothelial dysfunction and hypertension in mice in vivo. *Circulation* 2014;129:1428–1439
30. Zhou J, Wang Q, Ding Y, Zou MH. Hypochlorous acid via peroxynitrite activates protein kinase C θ and insulin resistance in adipocytes. *J Mol Endocrinol* 2015;54:25–37
31. Torres G, Morales PE, García-Miguel M, et al. Glucagon-like peptide-1 inhibits vascular smooth muscle cell dedifferentiation through mitochondrial dynamics regulation. *Biochem Pharmacol* 2016;104:52–61
32. Xie Z, Lau K, Eby B, et al. Improvement of cardiac functions by chronic metformin treatment is associated with enhanced cardiac autophagy in diabetic OVE26 mice. *Diabetes* 2011;60:1770–1778
33. Manucha W, Ritchie B, Ferder L. Hypertension and insulin resistance: implications of mitochondrial dysfunction. *Curr Hypertens Rep* 2015;17:504
34. Thomas SR, Witting PK, Drummond GR. Redox control of endothelial function and dysfunction: molecular mechanisms and therapeutic opportunities. *Antioxid Redox Signal* 2008;10:1713–1765
35. Willems PH, Rossignol R, Dieteren CE, Murphy MP, Koopman WJ. Redox Homeostasis and Mitochondrial Dynamics. *Cell Metab* 2015;22:207–218
36. Davidson SM, Duchon MR. Endothelial mitochondria: contributing to vascular function and disease. *Circ Res* 2007;100:1128–1141
37. Devarajan A, Bourquard N, Hama S, et al. Paraoxonase 2 deficiency alters mitochondrial function and exacerbates the development of atherosclerosis. *Antioxid Redox Signal* 2011;14:341–351
38. Kukidome D, Nishikawa T, Sonoda K, et al. Activation of AMP-activated protein kinase reduces hyperglycemia-induced mitochondrial reactive oxygen species production and promotes mitochondrial biogenesis in human umbilical vein endothelial cells. *Diabetes* 2006;55:120–127
39. Fujisawa K, Nishikawa T, Kukidome D, et al. TZDs reduce mitochondrial ROS production and enhance mitochondrial biogenesis. *Biochem Biophys Res Commun* 2009;379:43–48
40. Forouzanfar F, Salazar G, Patrushev N, et al. Metformin beyond diabetes: pleiotropic benefits of metformin in attenuation of atherosclerosis. *J Am Heart Assoc* 2014;3:e001202
41. Vasamsetti SB, Karnewar S, Kanugula AK, Raj AT, Kumar JM, Kotamraju S. Metformin inhibits monocyte-to-macrophage differentiation via AMPK-mediated inhibition of STAT3 activation: potential role in atherosclerosis. *Diabetes* 2015;64:2028–2041
42. Zhang L, Ji L, Tang X, et al. Inhibition to DRP1 translocation can mitigate p38 MAPK-signaling pathway activation in GMC induced by hyperglycemia. *Ren Fail* 2015;37:903–910
43. Huang S, Wang Y, Gan X, et al. Drp1-mediated mitochondrial abnormalities link to synaptic injury in diabetes model. *Diabetes* 2015;64:1728–1742
44. Men X, Wang H, Li M, et al. Dynamin-related protein 1 mediates high glucose induced pancreatic beta cell apoptosis. *Int J Biochem Cell Biol* 2009;41:879–890
45. Schulz E, Anter E, Zou MH, Keaney JF Jr. Estradiol-mediated endothelial nitric oxide synthase association with heat shock protein 90 requires adenosine monophosphate-dependent protein kinase. *Circulation* 2005;111:3473–3480
46. Davis BJ, Xie Z, Viollet B, Zou MH. Activation of the AMP-activated kinase by antidiabetes drug metformin stimulates nitric oxide synthesis in vivo by promoting the association of heat shock protein 90 and endothelial nitric oxide synthase. *Diabetes* 2006;55:496–505
47. Chen Z, Peng IC, Sun W, et al. AMP-activated protein kinase functionally phosphorylates endothelial nitric oxide synthase Ser633. *Circ Res* 2009;104:496–505
48. Egan DF, Shackelford DB, Mihaylova MM, et al. Phosphorylation of ULK1 (hATG1) by AMP-activated protein kinase connects energy sensing to mitophagy. *Science* 2011;331:456–461
49. The Expert Committee on the Diagnosis and Classification of Diabetes Mellitus. Report of the Expert Committee on the Diagnosis and Classification of Diabetes Mellitus. *Diabetes Care* 1997;20:1183–1197
50. Toyama EQ, Herzig S, Courchet J, et al. AMP-activated protein kinase mediates mitochondrial fission in response to energy stress. *Science* 2016;351:275–281
51. Gray SP, Di Marco E, Okabe J, et al. NADPH oxidase 1 plays a key role in diabetes mellitus-accelerated atherosclerosis. *Circulation* 2013;127:1888–1902
52. Sharma A, Sellers S, Stefanovic N, et al. Direct endothelial nitric oxide synthase activation provides atheroprotection in diabetes-accelerated atherosclerosis. *Diabetes* 2015;64:3937–3950